J Appl Electrochem (2008) 38:703–712
DOI 10.1007/s10800-008-9495-5

ORIGINAL PAPER

Photoelectrocatalytic activity of mesoporous TiO_2 films prepared using the sol–gel method with tri-block copolymer as structure directing agent

W. Y. Gan · M. W. Lee · R. Amal · H. Zhao · K. Chiang

Received: 5 October 2007 / Revised: 21 January 2008 / Accepted: 21 January 2008 / Published online: 5 February 2008

Abstract Mesoporous TiO_2 films were synthesized using a sol–gel process with a tri-block copolymer (Pluronic F127) as a structure directing agent. The films were dip-coated onto conductive glass substrates followed by thermal treatment to remove the polymeric surfactant. The specific surface area, the pore size and morphology, and the crystallinity of the films were characterized. The analysis showed the structural properties of the films could be tailored by varying the surfactant concentration as well as the annealing temperature. The photocurrent responses of the prepared films were measured using a three-electrode photoelectrochemical cell in the presence of oxalic acid. When annealed at 450 °C, the dense electrode (control sample) had the strongest photoelectrocatalytic oxidation aptitude toward oxalic acid. The lower photocurrent response of the mesoporous electrodes compared to the dense electrode can be explained by poor inter-particle connectivity within the mesoporous TiO_2 network, leading to high electron transport resistance. The mesoporous electrode annealed at 550 °C, with improved connectivity, outperformed the dense electrode at a high oxalic concentration, as the lower surface area of the dense electrode restricted photoelectrocatalysis reactions on the surface. A further increase in annealing temperature to 650 °C resulted in a poor photocurrent response as the significant decrease in surface area outweighed the beneficial effect of improved connectivity.

W. Y. Gan · M. W. Lee · R. Amal (✉) · K. Chiang
ARC Centre of Excellence for Functional Nanomaterials, School of Chemical Sciences and Engineering, The University of New South Wales, Sydney, NSW 2052, Australia
e-mail: r.amal@unsw.edu.au

H. Zhao
Australian Rivers Institute, Griffith School of Environment, Griffith University, Gold Coast Campus, QLD 4222, Australia

Keywords TiO_2 film · Mesoporous · Photoelectrocatalytic oxidation · Oxalic acid

1 Introduction

Titanium dioxide (TiO_2) is a semiconductor photocatalyst widely used in dye-sensitized solar cells, sensors, self-cleaning surfaces, and electrochromic devices. It is a promising photocatalyst for remediation of organic pollutants in air [1–3] and water [4–7]. Compared with TiO_2 suspension, immobilized TiO_2 photocatalysis requires no post-separation but exhibits surface area constraints. Methods available for the preparation of TiO_2 films include sputtering [8], chemical vapor deposition [9], spray pyrolysis [10] and sol–gel deposition [11, 12]. The most commonly employed method is the sol–gel technique due to its simplicity. The morphology, particle size, and crystalline phase of the constituent colloids assembling the films, as well as their porosity and surface area, are known to influence catalytic activity.

Recently, focus on TiO_2 film fabrication has shifted to controlling the pore volume and pore size of the semiconductor network [13–17]. Polymeric surfactants are used as structure directing agents to fabricate the desired mesoporous architecture. Subsequent removal of the polymeric contents via solvent extraction or thermal treatment results in a material possessing large effective surface areas, pore volumes and controllable pore sizes [13–17]. These structural characteristics improve light absorption efficiency and facilitate reactant and product transport into and out of the film network, consequently enhancing photoactivity and quantum efficiency [18, 19]. Zhang et al. [19] reported an improved photocatalytic activity of mesoporous films due to an enlarged surface area. The highly porous film was able to

degrade aqueous rhodamine B and gaseous formaldehyde twenty-two and six times faster, respectively, compared with a dense film [19]. Choi et al. [20] also prepared mesoporous TiO_2 films by incorporating polyethylene glycol sorbitan monolaurate (Tween-80) during the synthesis. The authors obtained highly porous TiO_2 films which displayed four times higher photoactivity for the decolorization of methylene blue, compared with the dense film [20].

Despite the recognized benefits of mesoporous TiO_2 films for photocatalysis, studies on mesoporous films for photoelectrocatalytic processes are limited. Little is known regarding the influence of porosity on photoelectrocatalytic activity and it is difficult to directly extrapolate known characteristics of photocatalysis to photoelectrocatalysis as the charge transfer mechanisms involved in both processes differ. In particular, connectivity of the porous semiconductor network plays an important role in photoelectron-capturing efficiency due to the applied potential bias, which in turn governing the overall effectiveness of the photoelectrocatalytic process. Zukalová et al. [21] reported an approximately 50% enhancement in solar conversion efficiency by a Pluronic P123-templated mesoporous TiO_2 film compared with a film comprising randomly associated TiO_2 particles and of similar thickness. They attributed this to the markedly enhanced surface area of the mesoporous film as the semiconductor was readily accessible to both the dye and the electrolyte. Although the electron injection mechanism of a dye-sensitized solar cell differs from a photoelectrocatalytic process, both possess very similar electron transport mechanisms inside the semiconductor layer, which is one of the factors affecting their photoefficiency. However, the selection of TiO_2 films synthesis conditions to provide optimum photoelectrocatalytic activity would depend on the chemical structure of the target organic reactant as the oxidation mechanisms are not universal [22, 23].

The present study investigates the effects of surfactant concentration and thermal treatment temperature on the physicochemical properties and the photocurrent response of mesoporous TiO_2 films. The films were prepared via the sol–gel process in the presence of a high molecular weight tri-block copolymer, Pluronic F127 ($EO_{106}PO_{70}EO_{106}$). The photocurrents obtained in the presence of oxalic acid were used to evaluate the photoelectrocatalytic activity of these films.

2 Experimental

2.1 Materials

Indium tin oxide (ITO) conducting glass slides were purchased from Delta Technologies Ltd. (USA). Titanium (IV) tetraisopropoxide (97%, Aldrich), isopropanol (99.5%, Ajax), oxalic acid (Ajax) and $NaClO_4$ (Ajax) were used as received. Distilled water (Millipore, Milli-Q Plus) was used for preparing all solutions. The pH of the solution was adjusted either with NaOH or $HClO_4$.

2.2 Mesoporous TiO_2 electrodes preparation

TiO_2 colloid was prepared according to the method described by Nazeeruddin et al. [24]. Titanium (IV) tetraisopropoxide in isopropanol was dripped into 0.1 M nitric acid solution under vigorous stirring. Following hydrolysis, the slurry was heated in a water bath to 80 °C and stirred vigorously for 12 h to disperse agglomerates. The slurry was autoclaved for 12 h at 200 °C. The final solid concentration of the colloid was approximately 3.5 wt% TiO_2.

To generate mesoporous structures, tri-block copolymer Pluronic F127 was added to the TiO_2 colloid and stirred for 2 h. The amount of added surfactant varied with the molar concentration of the titanium (Ti), giving F127 to Ti percentages of 0.25, 0.50, 0.75 and 1.00%. Single coating of the TiO_2 film was deposited on conductive glass substrates by a dip-coater with dropping speed of 0.20 cm s^{-1}, raising speed of 0.23 cm s^{-1} and dipping time of 30 s. Following the coating process, the films were dried at 25 °C and a relative humidity of 40% for 24 h. Controlled heating of the coated ITO substrates was carried out at 40 °C for 24 h and then at 110 °C for 24 h to enhance the inorganic polymerization and stabilize the mesophases. The films were annealed in a muffle furnace at 450, 550 or 650 °C for 30 min (in air with a ramp rate of 3 °C min^{-1}) to remove the organic template. The dense films (control samples) were prepared according to the same procedure without the addition of surfactant.

2.3 Electrode characterization

The crystalline structure of the TiO_2 network was analyzed by a Philips X'Pert MRD X-ray diffractometer, using graphite monochromatic copper radiation (Cu K_α). The films were scanned in a step mode at a step size of 0.2° and scan rate of 0.05° 2θ s^{-1}. The accelerating voltage and applied current were 45 kV and 40 mA, respectively. Crystalline phase identification was performed using PANalytical X'Pert Highscore Plus software.

The low surface area of films meant their specific surface area could not be determined accurately by conventional N_2 adsorption apparatus. Physicochemical sorption properties and pore parameters of powder samples prepared in an identical manner as the films were analyzed by N_2 adsorption–desorption at 77 K by the Micromeritics

Tristar 3000. All samples were degassed at 150 °C prior to surface area measurement. The surface morphology of the TiO_2 films were analyzed with a Hitachi S900 field-emission scanning electron microscope (FESEM).

2.4 Photoelectrochemical measurements

Photoelectrochemical measurements were carried out in a three-electrode electrochemical cell containing 100 cm^3 of 0.1 M $NaClO_4$ electrolyte with a quartz window for illumination. The exposed area of the working TiO_2 electrode for UV illumination and photoelectrochemical reaction was 0.79 cm^2. A saturated Ag/AgCl electrode and a platinum plate were used as the reference and the auxiliary electrodes, respectively. An Autolab potentiostat (PGSTAT12) was used for linear potential sweep measurements. The pH of the solution was adjusted to 6.00 ± 0.05 at the beginning of all experiments. UV illumination was provided by an assembly comprising of a 150 W Xenon arc lamp light source and focusing lenses (Beijing Optical Instruments). In conjunction with a band pass filter (UG-5, Schott), the assembly provided UV irradiation in 230–400 nm at an intensity of 6.0 mW cm^{-2}, as measured with an International Light Inc. model IL 1400A photometer (UVA#27359).

3 Results and discussion

3.1 Morphological and structure properties

3.1.1 Effect of surfactant concentration

Figure 1 shows the N_2 adsorption–desorption isotherms of mesoporous TiO_2 films prepared at different surfactant concentrations. All samples yielded Type IV isotherms with a small degree of hysteresis. According to the IUPAC classification, the hysteresis loops in Fig. 1 correspond to Type H2, which represents poorly defined pore size and shape distributions [25]. The dense sample had the lowest specific surface area and pore volume. Surface area and pore volume increased with surfactant addition. The 0.50%

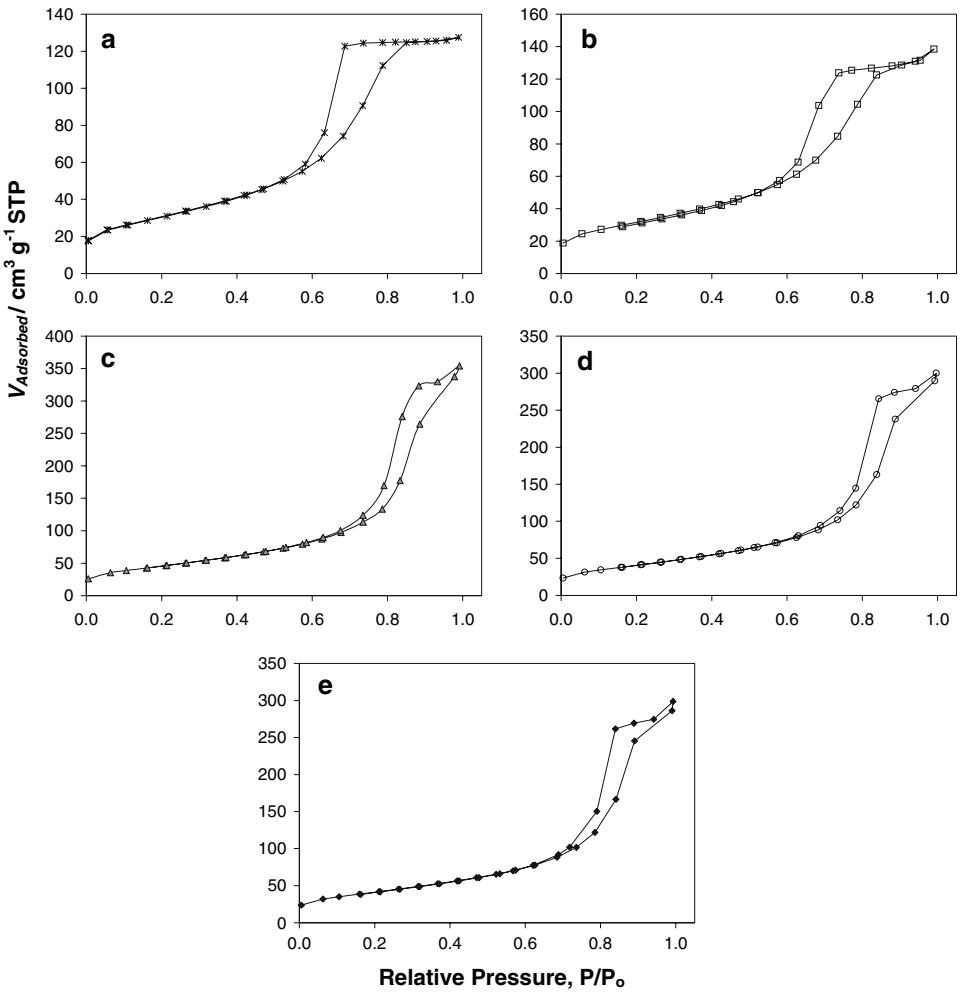

Fig. 1 N_2 adsorption–desorption isotherms of mesoporous TiO_2 powders with different F127/Ti molar percentages: (**a**) no surfactant; (**b**) 0.25; (**c**) 0.50; (**d**) 0.75; (**e**) 1.00% films annealed at 450 °C

F127/Ti sample displayed the highest specific surface area 165 m^2 g^{-1} and the highest pore volume 0.55 cm^3 g^{-1}. The high specific surface area and pore volume may be associated with the formation of larger mesopores [26]. As shown in Fig. 2, surfactant addition gave a broader pore diameter distribution and increased the average pore size from 5.9 nm (dense sample) to 10.5 nm. When the F127/Ti percentage increased beyond 0.50%, a decrease in the surface area was observed. A summary of the specific surface area and pore properties for all the TiO_2 samples is provided in Table 1.

Figure 3 shows the FE-SEM images of the mesoporous TiO_2 films annealed at 450 °C. The dense film comprises a flat and compact surface morphology (Fig. 3a). With the addition of surfactant, the films exhibit a more open structure. The formation of secondary clusters from the aggregation of primary particles was observed. The original size of the primary particles was estimated to be 10 nm from TEM micrographs.

XRD patterns obtained from the mesoporous TiO_2 films with different F127/Ti molar percentages are shown in Fig. 4. All the samples consist of predominantly anatase with a small amount of brookite. Each spectra posses four crystal peaks at 25.3°, 37.8°, 48.1° and 55.1°, characteristic of the anatase phase, while a minor peak (30.8°) which can be assigned to the brookite phase was also visible in the pattern. No rutile peaks were evident in the spectra. Peaks at 35.5° and 50.9° were ascribed to indium oxide of the ITO glass.

Table 1 BET surface area and average pore size of TiO_2 samples prepared with different F127/Ti molar percentages and annealed at different temperatures

F127/Ti molar percentage (%)	Annealing temperature (°C)	BET surface area (m^2 g^{-1})	Average pore size (nm)
No surfactant	450	110	5.9
0.25	450	128	7.9
0.50	450	165	10.5
0.75	450	147	9.6
1.00	450	149	10.0
No surfactant	550	54	8.5
0.50	550	101	12.0
No surfactant	650	12	25.6
0.50	650	57	15.1

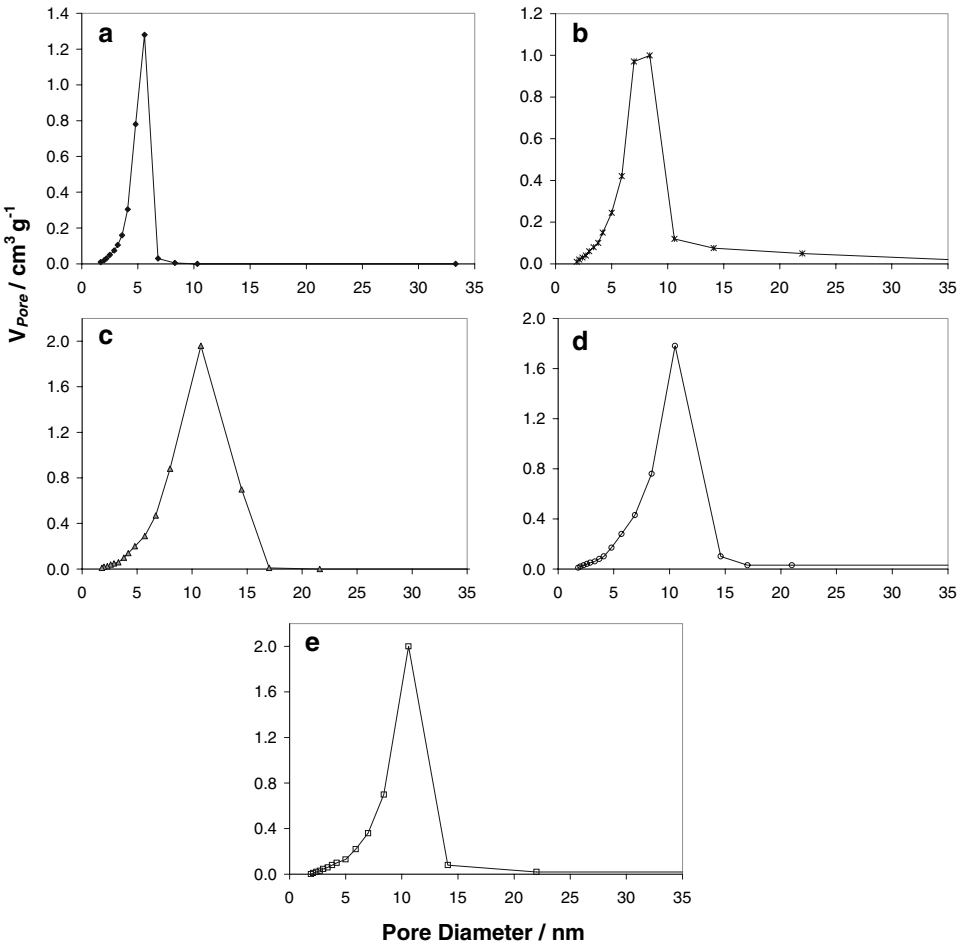

Fig. 2 Pore size distribution curves for mesoporous TiO_2 powders with different F127/Ti percentages: (**a**) no surfactant; (**b**) 0.25; (**c**) 0.50; (**d**) 0.75; (**e**) 1.00% samples annealed at 450 °C

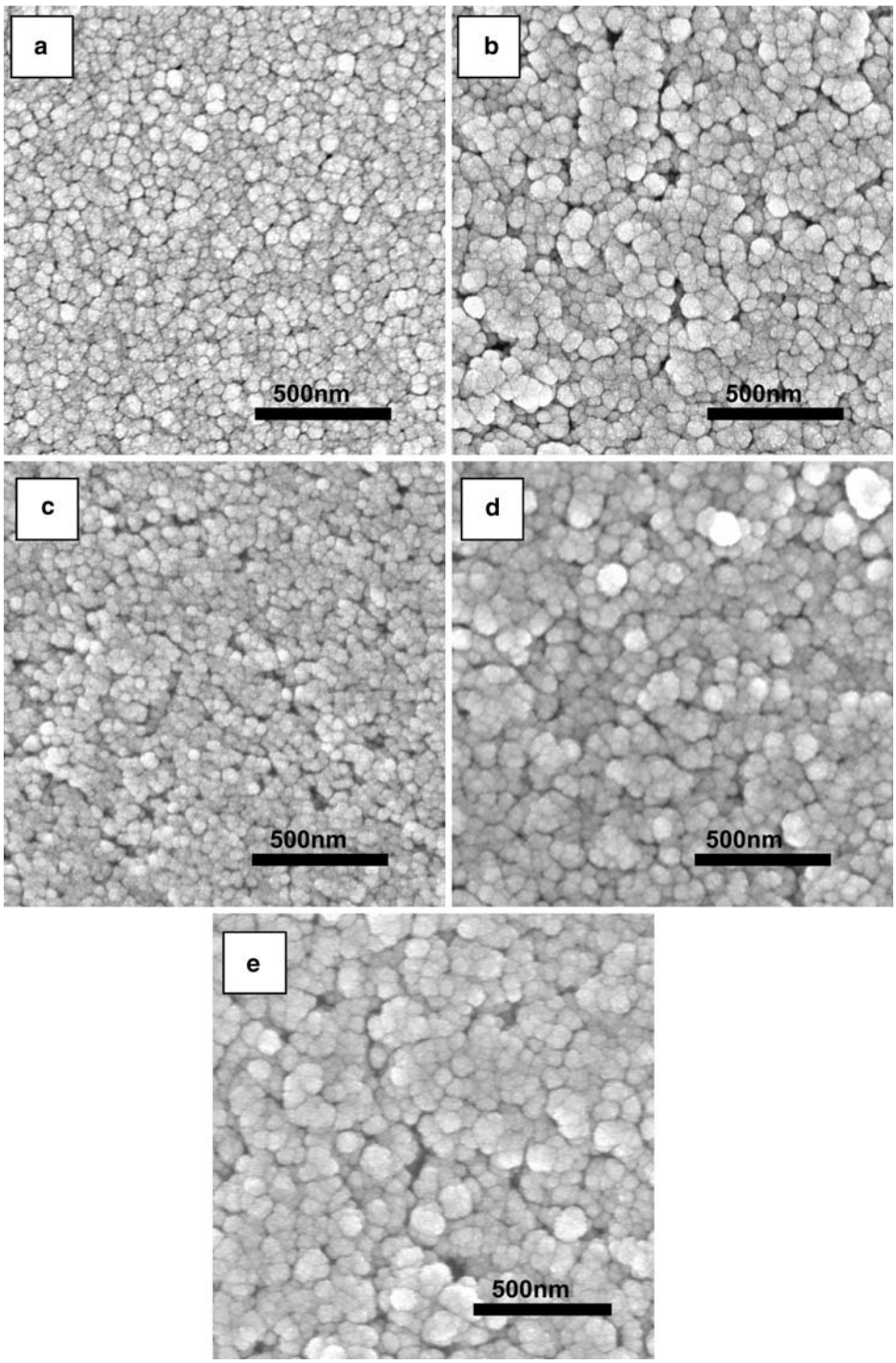

Fig. 3 FE-SEM images of mesoporous TiO_2 films with different F127/Ti molar percentages: (**a**) no surfactant, (**b**) 0.25; (**c**) 0.50%; (**d**) 0.75%; (**e**) 1.00% films annealed at 450 °C

3.1.2 Effect of annealing temperature

To investigate the effect of annealing temperature on structural characteristics of the mesoporous films, samples with 0.50% F127/Ti were calcined at 550 and 650 °C. Figure 5 shows the N_2 adsorption isotherm plots of the samples and Fig. 6 illustrates their pore size distributions. The samples displayed type IV isotherms, but contained different hysteresis patterns. The specific surface area of the mesoporous and dense samples decreased with increasing annealing temperature. The decreasing in specific surface area may be related to inter-crystallite sintering or/and intra-cluster densification into larger clusters [27]. Sintering leads to the elimination of small

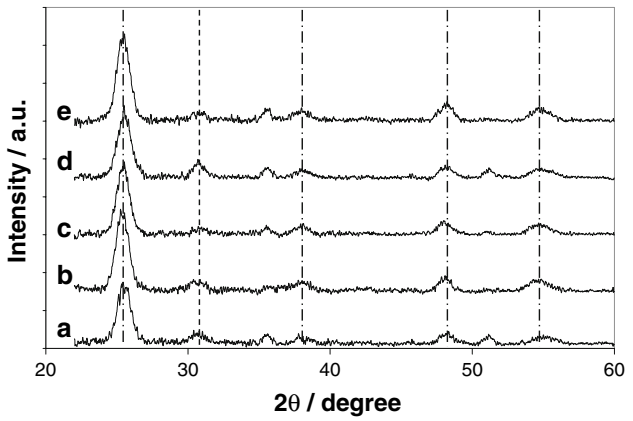

Fig. 4 XRD patterns of mesoporous TiO_2 films with different F127/Ti molar percentages: (**a**) no surfactant; (**b**) 0.25%; (**c**) 0.50%; (**d**) 0.75%; (**e**) 1.00% films annealed at 450 °C. The dash-dot lines represent anatase peaks as the dash line represents brookite peak

inter-crystallite pores and resulting in an increase in pore size and a decrease in the specific surface area. The higher annealing temperature also caused significant broadening of pore size distribution of the dense samples.

Figure 7 shows FE-SEM images of the TiO_2 films annealed at 550 and 650 °C. The film annealed at 550 °C (Fig. 7a) displayed a denser morphology than when annealed at 450 °C (Fig. 3c). At 650 °C, the size of the secondary clusters was much larger and the clusters undergoing further agglomeration. This demonstrates that primary particle agglomeration and sintering of secondary clusters becomes more profound with an increase in annealing temperature.

XRD patterns of the mesoporous TiO_2 films synthesized at 0.50% F127/Ti and annealed at different temperatures are shown in Fig. 8. Based on the peak intensity of anatase and brookite, at $2\theta = 25.38°$ and 30.76°, respectively, the anatase content of the samples was calculated according to Eq. 1:

$$\text{anatase}(\%) = \frac{100}{1 + 4.029(I_{\text{brookite}}/I_{\text{anatase}})} \quad (1)$$

where I_{brookite} and I_{anatase} are the intensities of the corresponding XRD signals.

The result indicated 72.8% of anatase was present in the sample annealed at 450 °C. Upon increasing the annealing temperature to 550 °C, the anatase peak intensity increased, while the brookite peak decreased slightly. The percentage of anatase in this sample increased to 83.0%. Increasing the annealing temperature to 650 °C increased anatase peak further, giving 88.4% of anatase in the sample.

3.2 Photoelectrochemical properties

3.2.1 Effect of surfactant concentration

Figure 9 shows the linear scan voltammograms obtained from the dense film annealed at 450 °C in 0.1 M $NaClO_4$ solution containing different oxalic acid concentrations. Oxalic acid was selected as the model organic compound for the photoelectrochemical studies as it is known to rapidly oxidize to carbon dioxide under the experimental conditions due to its simple molecular structure [5]. Figure 9 reveals

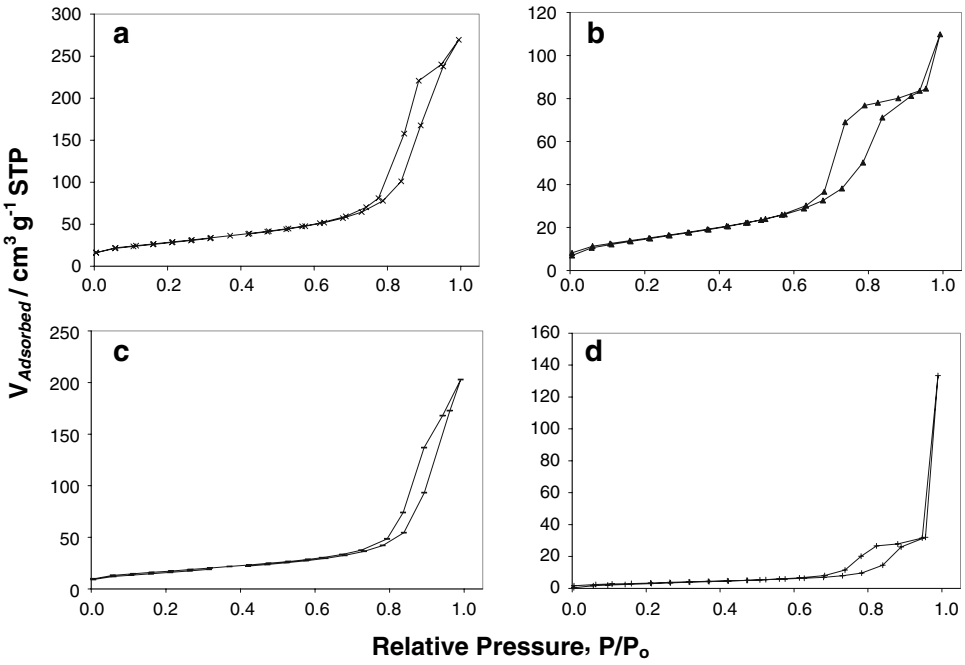

Fig. 5 N_2 adsorption–desorption isotherms of TiO_2 powders annealed at (**a**) 550 °C with F127, (**b**) 550 °C without F127, (**c**) 650 °C with F127, and (**d**) 650 °C without F127

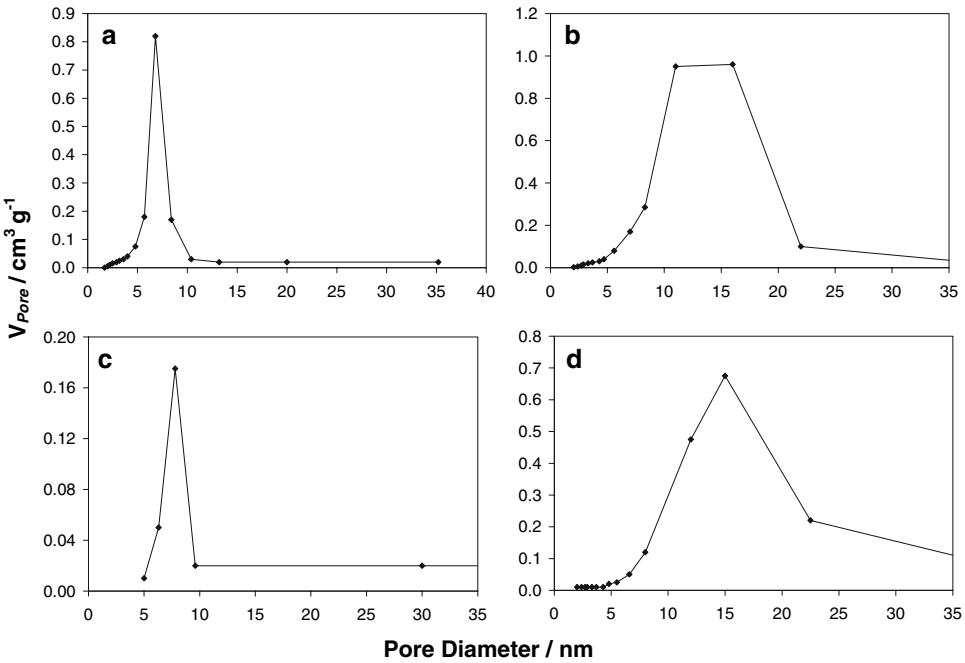

Fig. 6 Pore size distribution curves of TiO_2 powders annealed at (**a**) 550 °C with F127, (**b**) 550 °C without F127, (**c**) 650 °C with F127, and (**d**) 650 °C without F127

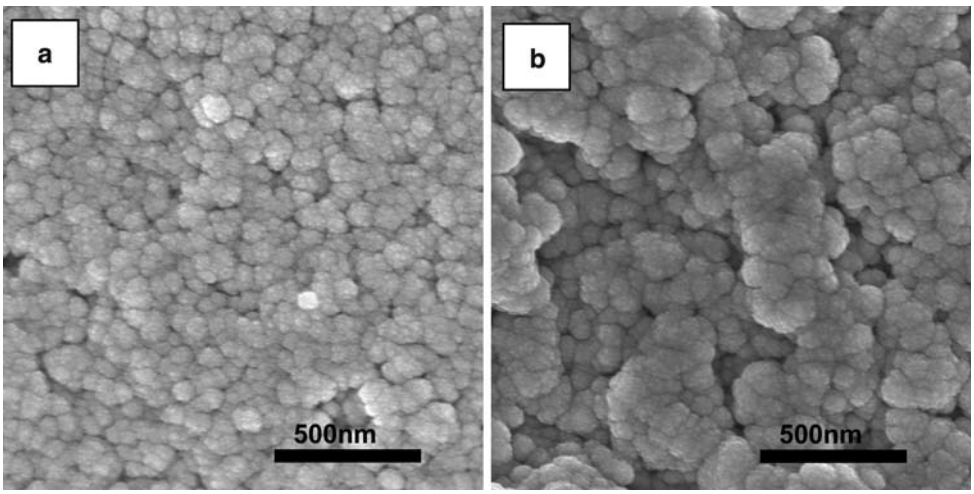

Fig. 7 FE-SEM images of mesoporous 0.50% F127/Ti TiO_2 films annealed at (**a**) 550 and (**b**) 650 °C

that for all cases, the photocurrent increases linearly with applied potential and is saturated at applied potentials of more positive than −0.2 V (versus Ag/AgCl reference) and is a typical I-E profile reported in previous studies [28–30]. The saturated photocurrent, I_{sph} represents the maximum photohole capture rate at the interface by oxalic acid and/or water molecules (in the absence of oxalic acid) [31]. In the absence of UV illumination, no significant current was detected. The characteristics of the voltammograms obtained from different electrodes listed in Table 1 were qualitatively similar to that shown in Fig. 9. The saturated photocurrent shifted to a higher value as the concentration of oxalic acid increased.

Figure 10 shows the plot of saturated photocurrent as a function of oxalic acid concentration. They indicate the I_{sph} increases linearly with oxalic acid concentration for all electrodes investigated when the concentration level is below 0.5 mM (see Fig. 10a). However, the dense TiO_2 electrode (control sample) and the mesoporous electrodes behaved differently at high concentration range. The I_{sph} of the dense TiO_2 electrode leveled off at high concentrations, while the photocurrents obtained for all mesoporous electrodes continued to increase linearly (within a medium-high concentration range 5–100 mM) but at a slower rate. The linear I_{sph}-concentration relationship obtained at the low concentration range for all electrodes was due to the system being under diffusion controlled conditions. Under these conditions, the limiting saturated photocurrent (I_{sph}) can be expressed by a semi-empirical equation (Eq. 2), provided all the organic molecules reaching the electrode

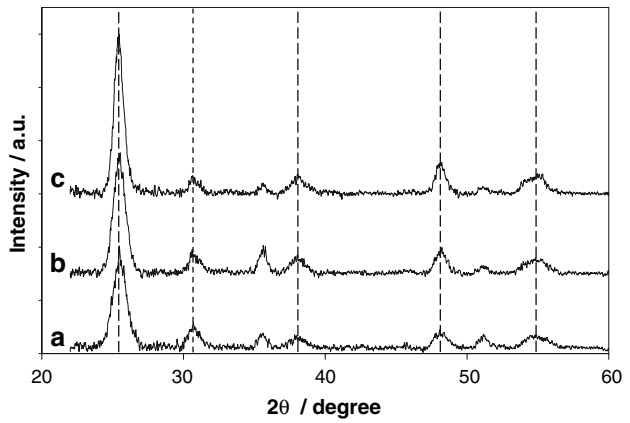

Fig. 8 XRD patterns of mesoporous TiO_2 films at 0.50% F127/Ti and annealed at (**a**) 450, (**b**) 550 and (**c**) 650 °C. The dash-dot lines represent anatase peaks as the dash line represents brookite peak

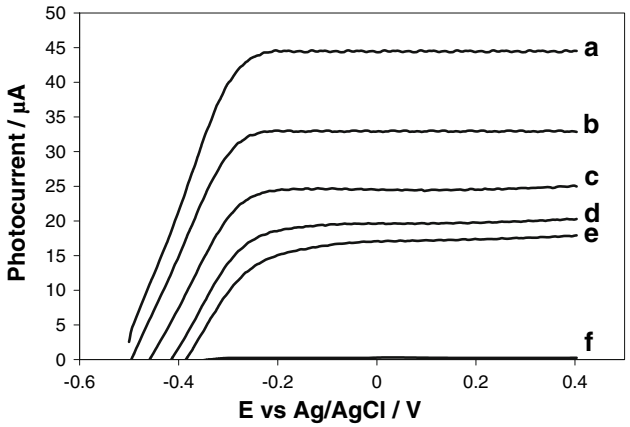

Fig. 9 Linear sweep voltammograms of dense TiO_2 film in 0.1 M $NaClO_4$ solution containing different oxalic acid concentrations. Oxalic acid concentration (**a**) 0.5; (**b**) 0.3; (**c**) 0.15; (**d**) 0.05; (**e**) 0.0; (**f**) 0.0 mM under non-illuminated conditions. Film annealed at 450 °C; Scan rate 10 mV s^{-1}

surface are stoichiometrically mineralized and all photoelectrons generated from the photocatalytic oxidation are collected (100% photoelectron collection efficiency) [32]:

$$I_{\text{sph}} = \frac{nFADC}{\delta} \tag{2}$$

where n is the number of electrons transferred for the complete mineralization of an organic compound, F is the Faraday constant, A is the effective surface area of the electrode, D is the diffusion coefficient of the compound, δ is the thickness of the Nernst diffusion layer and C is the bulk concentration of the compound.

Slopes of the linear curves ($nFDA/\delta$) obtained from Eq. 2 can be collectively used to represent the photoelectrocatalytic oxidation performance of the electrodes [32]. In Fig. 10a the dense TiO_2 electrode exhibited the highest slope (52 μA mM^{-1}) with the slopes obtained for the

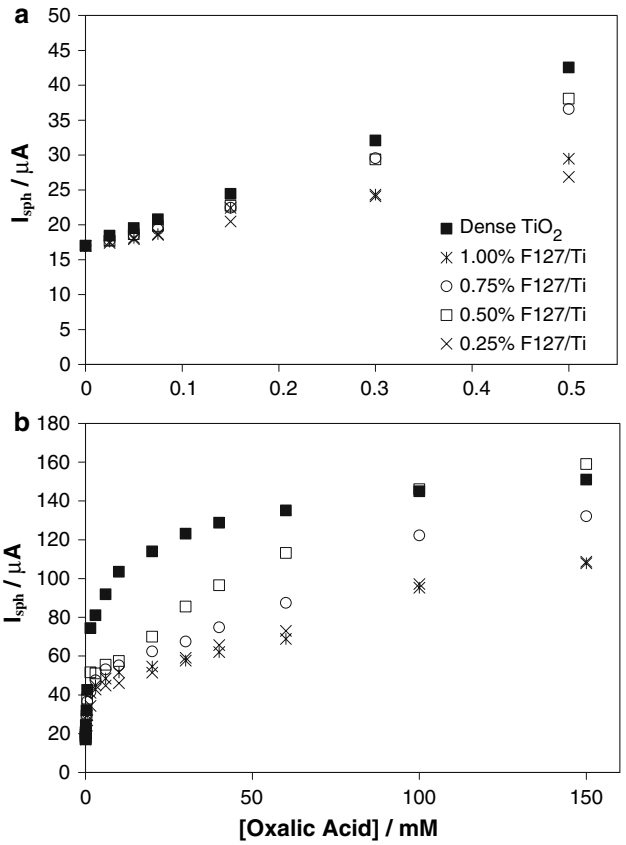

Fig. 10 Saturated photocurrent as a function of oxalic acid concentration for mesoporous TiO_2 electrodes prepared using different F127/Ti molar percentages and annealed at 450 °C: (**a**) at a lower organic concentration range (0.5 mM) and (**b**) at a higher concentration range (150 mM). Saturated photocurrent taken at +0.3 V applied potential

mesoporous electrodes lower and varied with surfactant concentration. The high slope obtained for the dense electrode can be attributed to its compact structure giving superior connectivity between the particles. This indicates optimal structural characteristics are critical for high photoelectron collection efficiency. The slopes obtained for the mesoporous electrodes increased as the specific surface area of the electrodes increased, which is in agreement with Eq. 2. A porous structure is favorable for heterogeneous photocatalysis reactions, as the large surface area facilitates organic adsorption and promotes surface reactions. Reactants and products are permitted to diffuse into and out of the electrode surfaces swiftly during the photoelectrocatalytic reactions due to the increase in surface reaction sites [18].

Deviation from the linear relationship at higher organic concentrations can be attributed to the accumulation of organic molecules and/or their intermediates on the surface of the electrodes. The available photoholes are insufficient to completely oxidize the organic molecules. At this condition, photohole generation (light intensity) becomes the limiting step of the overall reaction [32]. For the dense

electrode, I_{sph} reached a saturation level at high oxalic acid concentrations, indicating the photoelectrocatalytic oxidation of oxalic acid had reached its limiting point. Increasing the amount of oxalic acid and its partial degraded intermediates in the reaction zone did not further facilitate the photohole capture process. Conversely, the monotonic increase of I_{sph} with organic concentration even at high oxalic concentrations for the mesoporous electrodes suggests that the organic compound and its partially-degraded intermediates have not saturated the mesoporous surface due to the enlarged surface area and porous nature of the electrodes. Moreover, the enhancement in light harvesting by the multiple scattering of the porous network [33] may also contribute to the difference in I_{sph}-concentration profile.

3.2.2 *Effect of annealing temperature*

TiO_2 films were annealed at temperatures higher than 450 °C to improve the inter-particle network and therefore the connectivity between the grain particles. However, several intrinsic changes to the structural properties of the films also occurred during the annealing process. At higher annealing temperatures, the crystallinity of the TiO_2 particles improves and the number of defects is reduced [22, 23]. This results in a lower rate of photogenerated hole-electron recombination [22, 23]. The amount of brookite also decreased as the annealing temperature increased. A negative outcome of the higher annealing temperatures is the decrease in film surface area due to the collapse of small pores and the fusion of small crystallites into larger clusters.

Figure 11 shows the change in saturated photocurrent as a function of oxalic acid concentration for TiO_2 electrodes prepared at 0.50% F127/Ti and annealed at 450, 550 and 650 °C. The I_{sph} profiles exhibited by the mesoporous and dense electrodes again differed from each other in a similar way as described in Figure 10. In the low concentration range (<0.1 mM), the I_{sph} for all electrodes increased linearly with organic concentration. When the organic concentration was greater than 3 mM, significant differences in the I_{sph} profiles occurred. Over the concentration range 3–50 mM, the I_{sph} derived from oxalic acid oxidation decreased in the order: dense TiO_2 550 °C > 0.50% F127/Ti 550 °C > dense TiO_2 450 °C > 0.50% F127/Ti 450 °C > dense TiO_2 650 °C > 0.50% F127/Ti 650 °C. As mentioned previously, I_{sph} is controlled by electron injection at the TiO_2/solution interface as well as electron transport in the semiconductor film. Within this concentration range, the rate of electron transport inside the mesoporous films cannot reach a level comparable to the rate of photohole capture at TiO_2/solution interface and the observed photocurrent is limited by the electron transport

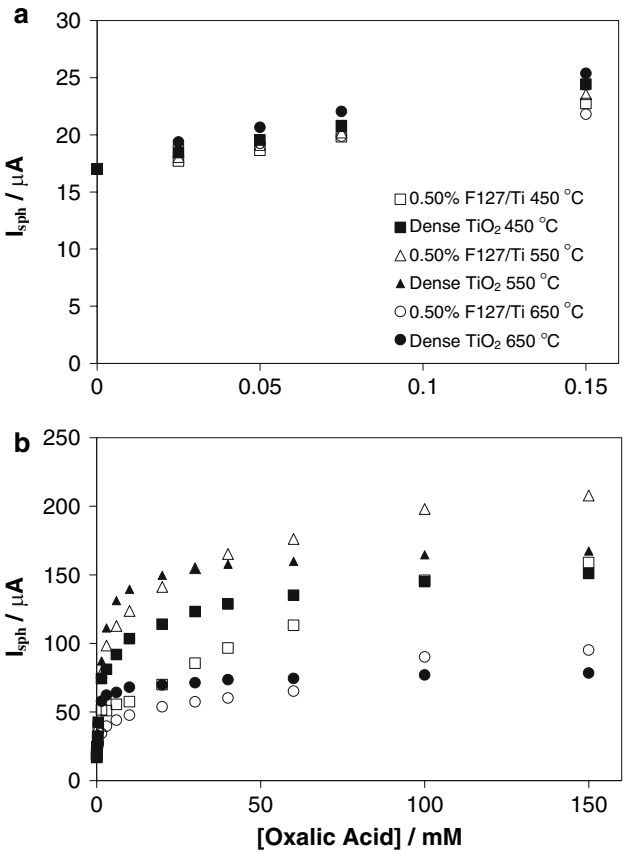

Fig. 11 Saturated photocurrent as a function of oxalic acid concentration for mesoporous TiO_2 electrodes prepared using 0.50% F127/Ti annealed at different temperatures: (**a**) at a lower organic concentration range (0.15 mM) and (**b**) at a higher concentration range (150 mM). Saturated photocurrent taken at +0.3 V applied potential

across the TiO_2 film. This means the electron-hole recombination rate resulting from poor connectivity is outweighed by the surface electron injection rate and restricts the photocurrent response of mesoporous films. Films annealed at 550 °C had a higher I_{sph} than films annealed at 450 and 650 °C. Beside improved connectivity, changes in crystal defect concentration might also be a contributing factor. Polycrystalline TiO_2 films have a considerable number of structural defects which are present as electron traps [5]. Photogenerated electrons have a tendency to fill these traps before being drawn to the ITO. The elimination of structural defects at higher annealing temperatures may provide a more direct electron path to the ITO and contribute to higher a I_{sph}. However, at 650 °C, the decrease in surface area dominates causing the drop in photocurrent response.

As the concentration of oxalic acid increased, the apparent oxidation level of the TiO_2 electrodes reversed in the sequence of (from highest to lowest): 0.50% F127/Ti 550 °C > dense TiO_2 550 °C > 0.50% F127/Ti 450 °C > dense TiO_2 450 °C > 0.50% F127/Ti 650 °C > dense

TiO_2 650 °C. The lower surface area of dense films restricts the photoelectrocatalysis reactions as the electrode surface is more readily saturated with the organic compound and its intermediates. This is reflected in the I_{sph} profile showing the photocurrents of all the dense films leveled off at high organic concentrations. On the other hand, the larger surface area of the mesoporous electrodes continues to allow adsorption of organic species to further facilitate the surface reactions. This rationalization is supported by the proposed mechanism for oxidation of strongly adsorbed oxalic acid molecules on TiO_2 [5]. Under these conditions, the rate of electron injection at the TiO_2/solution interface is overwhelmingly high and the high electron concentration gradient begins to force the electron cross the film resulting in a higher I_{sph}. Although the specific surface area of 0.50% F127/Ti 550 °C electrode was not as high as the 0.50% F127/Ti 450 °C electrode, the net effect of the improved interparticle connectivity, facilitates electron mobility acrossed the film, providing the optimum photoelectrocatalytic activity. The selection of synthesis conditions to provide optimum photoelectrocatalytic activity, however, depends on the target organic reactant.

4 Conclusions

Mesoporous TiO_2 electrodes were successfully prepared via the sol–gel process by using a tri-block copolymer, F127, as a structure-directing agent. The synthesized electrodes were found to have larger specific surface areas and higher porosities than the corresponding dense electrodes. At an annealing temperature of 450 °C, the oxidation aptitude of the dense electrode was superior to those of mesoporous electrodes due to the poor interparticle connection within the mesoporous TiO_2 network, leading to a high resistance to electron transport within the porous network. When the mesoporous electrode was annealed at 550 °C, the improved connectivity and enlarged surface area outperformed the dense electrode at high oxalic concentrations as the lower specific surface area of dense electrode was readily saturated. However, further increases in the annealing temperature to 650 °C resulted in poor photocurrent response, as the decrease in specific surface area was the dominant effect, outweighing the beneficial effect of improved connectivity. It was demonstrated that an optimal balance between mesoporous structure, crystallinity and structure connectivity is the key factor for photoelectrocatalytic performance. For the present system, TiO_2 mesoporous electrodes with an optimum performance can be prepared at 0.50% F127/Ti and at an annealing temperature of 550 °C.

Acknowledgements This work was carried out with financial assistance from the Australian Research Council Centre of Excellence for Functional Nanomaterials.

References

1. Young C, Lim TM, Chiang C, Scott J, Amal R (2008) Appl Catal B 78:1
2. Kim SB, Hwang HT, Hong SC (2002) Chemosphere 48:437
3. Hager S, Bauer R (1999) Chemosphere 38:1549
4. Jiang D, Zhao H, Zhang S, John R, Will GD (2003) J Photochem Photobiol A 156:201
5. Jiang D, Zhao H, Zhang S, John R (2004) J Catal 223:212
6. Bryne JA, Eggins BR, Brown NMD, McKinney B, Rouse M (1998) Appl Catal B 17:25
7. Selcuki H, Zaltner W, Sene JJ, Bekbolet M, Anderson MA (2004) J Appl Electrochem 34:653
8. Yoko T, Hu L, Kozuka H, Sakka S (1996) Thin Solid Films 283:188
9. Hidaka H, Ajisaka K, Horikoshi S, Oyama T, Takeuchi K, Zhao J, Serpone N (2001) J Photochem Photobiol A 138:185
10. Thybo S, Jensen S, Johansen J, Johannessan T, Hansen O, Quade U (2004) J Catal 223:271
11. Liu J, Yang DD, Shi F, Cai Y (2003) Thin Solid Films 429:225
12. Hattori A, Shimoda K, Tada H, Ito S (1999) Langmuir 15:5422
13. Antonelli DM, Ying JY (1995) Angew Chem Int Ed Engl 34:2014
14. Negishi N, Takeuchi K (2001) Thin Solid Films 392:249
15. Negishi N, Takeuchi K (2003) Res Chem Intermed 29:861
16. Negishi N, Matsuzawa S, Takeuchi K, Pichat P (2007) Chem Mater 19:3808
17. Yu JC, Wang XC, Wu L, Ho WK, Zhang LZ, Zhou GT (2004) Adv Funct Mater 14:1178
18. Antonietti M (2001) Curr Opin Colloid Interface Sci 6:244
19. Zhang L, Zhu Y, He Y, Li W, Sun H (2003) Appl Catal B Environ 40:287
20. Choi H, Stathatos E, Dionysiou DD (2006) Thin Solid Films 510:107
21. Zukalová M, Zukal A, Kavan L, Nazeeruddin MK, Liska P, Gratzel M (2005) Nano Lett 5:1789
22. Agrios AG, Pichat P (2006) J Photochem Photobiol A 180:130
23. Enríquez R, Agrios AG, Pichat P (2007) Catal Today 120:196
24. Nazeeruddin MK, Kay A, Rodicio I, Humphry-Baker R, Muller E, Liska P, Vlachopoulos N, Gratzel M (1993) J Am Chem Soc 115:6382
25. Lowell S, Shields JE, Thomas MA, Thommes M (2004) Characterisation of porous solids and powders: surface area, pore size and density, 4th edn. Kluwer Academic Publishers, Boston
26. Greg SJ, Sing KSW (1982) Adsorption, surface area and porosity, 2nd edn. Academic Press, London
27. Brinker CJ, Scherer GW (1990) Sol–gel science: the physics and chemistry of sol–gel processing. Academic Press, New York
28. Byrne JA, Eggins BR, Linquette-Mailley S, Dunlop PSM (1998) Analyst 123:2007
29. Bryne JA, Eggins BR (1998) J Electroanal Chem 457:61
30. Sodergren A, Hagfeldt A, Olsson J, Lindquist S (1994) J Phys Chem 98:5552
31. Jiang D, Zhao H, Zhang S, John R (2003) J Phys Chem B 107:12774
32. Jiang D, Zhao H, Zhang S, John R (2006) J Photochem Photobiol A 177:253
33. Hagfeldt A, Gratzel M (2000) Acc Chem Res 33:269